ADVANCED OPTICAL MATERIALS
www.advopticalmat.de

Narrow Linewidth Spontaneous and Lasing Emissions from Open-Access Microcavity-Embedded Perovskite Quantum Dots

*Sunny Tiwari, Amit R. Dhawan, SangHyuk Park, Sangeun Cho, Gareth S. Jones, Jason M. Smith, Robert A Taylor, and Tristan Farrow**

Achieving efficient optical coupling between the emission from perovskite quantum dots (PQDs) and photonic integrated elements requires ultranarrow linewidths and highly directional emission. These are challenging goals at room temperature due to the broad and isotropic nature of perovskite emission. Here, we demonstrate ultranarrow-linewidth emission from $CsPbBr_3$ PQDs at room temperature, in both spontaneous and stimulated regimes, by coupling to state-of-the-art open-access curved dielectric cavities under continuous wave excitation. The emission is confined to a single transverse electromagnetic mode of the cavity, achieving a remarkably narrow linewidth of 0.2 nm, ≈100× narrower than free-space emission in both the emission regime. Single-mode lasing from a small number of PQDs is observed, yielding a quality factor of ≈2590, among the highest reported for single-mode lasing. The open-access design enables precise tuning of cavity length and selective coupling of emitters in their native state, overcoming the limitations associated with closed and fixed-length vertical-cavity surface emitting laser geometries. The geometry's low divergence and tunability provide an efficient route for integrating perovskite emitters with on-chip photonic circuits, advancing their use in quantum and optoelectronic technologies.

1. Introduction

Narrow linewidth emission is essential for advancing on-chip nanophotonics and nano-optics, where precise control over light-matter interactions plays a critical role in integrated photonic circuits, light-emitting diodes (LEDs), and quantum technologies.[1,2] High spectral purity and directional emission[3] are key requirements for these applications, particularly in quantum communication and computing systems that rely on the efficient generation and manipulation of photons.[4,5] One compelling route for achieving these characteristics is through lasing,[6–9] where stimulated emission produces coherent, narrowband light with high intensity and directionality. However, achieving room-temperature lasing with high spectral purity remains a challenge due to the broad and isotropic nature of spontaneous emission.[10]

Emitters such as semiconductor quantum dots suffer from multiexciton emission,[11,12] while nitrogen vacancy centres in diamond are limited by phonon sidebands that degrade photon coherence.[13] Perovskite quantum dots (PQDs), by contrast, are low-cost, bright,[14] highly tunable in size and emission wavelength[15,16] chemically[17,18] to achieve single photon superradiance with a single emitter,[19] and bright excitonic lasing.[20] Although lasing from pristine PQDs has been demonstrated,[7,20] it typically requires expensive cryogenic temperatures and often results in multimode, non-directional emission, as the geometry itself forms the cavity and the emission wavevectors are broadly distributed. One approach to achieve efficient lasing is by coupling PQDs emission to optical cavities, such as whispering gallery modes (WGMs) and dielectric distributed Bragg reflector (DBR) based cavities to form vertical cavity surface emitting lasers (VCSELs). On one hand, WGMs cavities,[21] can improve PL emission but are challenging to use due to the difficulty in positioning the emitters precisely at the intensity maxima. However, large supraparticles formed from small semiconductor quantum dots (CdSe/CdS) can simultaneously act as both the lasing gain medium and the cavity, providing wavelength-tunable lasing emission simply by changing the excitation wavelength.[22,23]

S. Tiwari, A. R. Dhawan, S. Park, R. A Taylor, T. Farrow
Department of Physics
University of Oxford
Parks Road, Oxford OX1 3PU, UK
E-mail: tristan.farrow@cantab.net
S. Cho
Division of System Semiconductor
Dongguk University
Seoul 04620, South Korea
G. S. Jones, J. M. Smith
Department of Materials
University of Oxford
Oxford OX1 3PH, UK
T. Farrow
NEOM Education, Research, and Innovation sector
Tabuk 49643-9136, Saudi Arabia
The ORCID identification number(s) for the author(s) of this article can be found under https://doi.org/10.1002/adom.202501918

DOI: 10.1002/adom.202501918

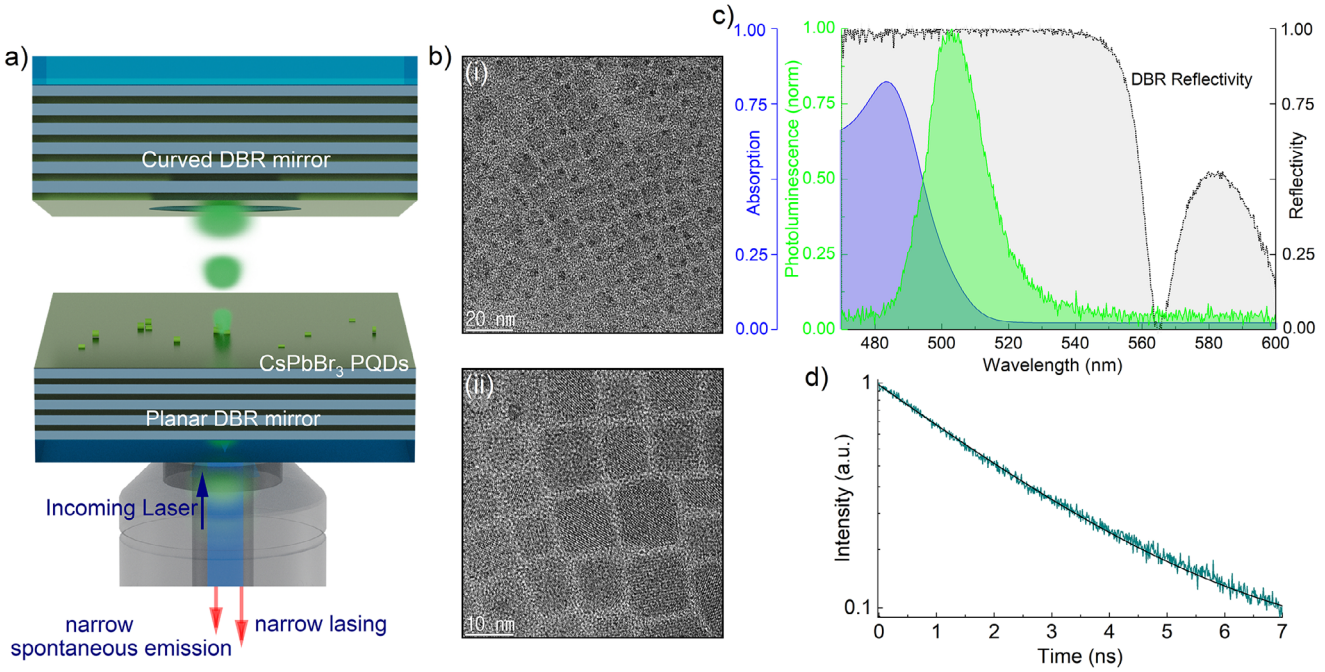

Figure 1. Experimental configuration. a) Schematic of the experimental configuration. Chemically synthesised $CsPbBr_3$ PQDs were spin-coated on a planar DBR mirror, which are coated with a reflectivity maximum at 510 nm. A small cluster of the PQDs was excited using a laser source, and emission was coupled to the Hermite–Gaussian modes of the open-access tunable dielectric optical cavity formed using a planar and a curved mirror. Spontaneous and stimulated emission coupled to a single TEM_{00} mode of the cavity was collected using the same objective lens. b) Transmission electron microscopy image of the monodispersed PQDs with a dimension of 10 nm edge size. c) Absorption (blue curve) and photoluminescence (green curve) spectra of the PQDs, and measured reflectivity (black curve) of the DBR mirrors. Room temperature out of cavity PL emission of the PQDs showing a broad linewidth with a FWHM of 19.0 ± 2.0 nm. d) Time-resolved photoluminescence measurement of the PQDs emission (cyan dots) and fitted curve (blue curve) showing a lifetime of 2.48 ± 0.26 ns.

Additionally, WGM cavities typically out-couple in a multimode regime,[24] which lacks the required directionality[25–27] for practical applications. On the other hand, most VCSEL geometries are closed structures,[28–30] which restrict tunability and reuse at different lasing wavelengths, and require high-power pulsed lasers to overcome the lasing threshold. These designs often have large cavity lengths,[28,30] which results in multimode outcoupling. Submicron length VCSELs[29] require embedding the emitters in polymer matrices to control the cavity thickness. More critically, the closed-cavity designs exhibit broad spontaneous emission spectra, necessitating threshold crossing to achieve narrow-linewidth emission, thus limiting their use for single-photon sources and cavity quantum electrodynamics at room temperature. Recently, small sized perovskite quantum dots have enabled the observation of polariton condensation in DBR based microcavities under pulsed excitation regimes.[31] To move beyond the limitations of pulsed excitation, there have been reports of continuous-wave (CW) lasing in solid-state perovskite microcavities.[32,33] However, these demonstrations typically rely on large micron scale perovskite structures or extended 2D films integrated with distributed feedback gratings,[34,35] which are less suitable for scalable single emitter integration or for realizing compact, wavelength tunable coherent light sources at room temperature.

To address these challenges, we use open-access dielectric cavities[36,37] with concave-plano mirror geometry,[38,39] which offer spectral tunability, straightforward alignment, and high-quality-factor single-mode emission with small mode volume. This architecture enables precise spatial positioning of the PQDs in their native state at the cavity mode to get ultra-narrow linewidth (0.2 nm) emission in both spontaneous and lasing regimes under CW pumping at room temperature. As a result, this platform provides a versatile solution that simultaneously supports fundamental studies, such as single-photon generation and coherent light-matter interaction, in the spontaneous regime, and enables practical applications like integrated nano-micro lasers and energy-efficient coherent sources in the stimulated regime.

2. Results and Discussion

Figure 1a shows the schematic of the experimental configuration. Chemically synthesised $CsPbBr_3$ PQDs[40] were spin-coated on a planar DBR mirror forming a distribution of single and small clusters of PQDs (see methods for details on preparation of PQDs, sample, and DBR mirrors). The concave mirror of the cavity was fabricated by milling a smooth micron-sized curved features using focused ion-beam (FIB) milling, which facilitates large Q values as well as ultra-small mode volume cavity resonances.[38,39,41] The DBR mirrors were created by coating 11 pairs of SiO_2 and Ta_2O_5 to get a reflectivity of >99.5% at a target wavelength of 510 nm, which is near the emission maxima of the PQDs. A small cluster of PQDs was excited using 405 nm CW, or pulsed laser source, and the PQD emission was coupled to the

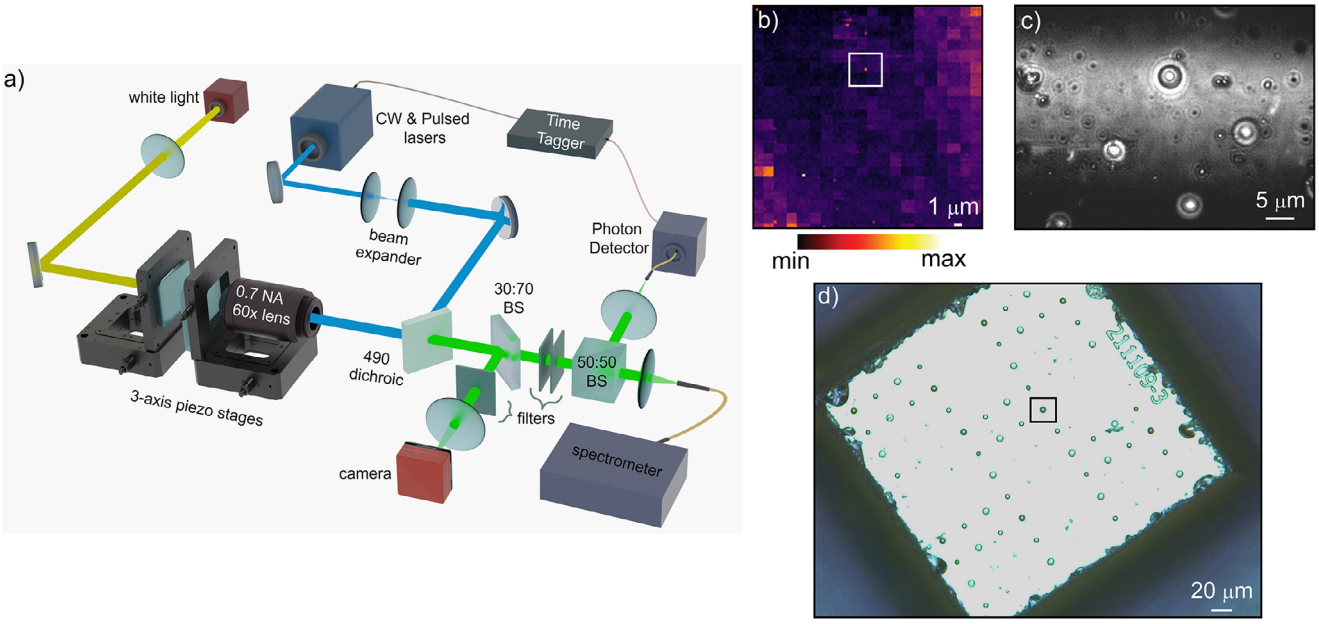

Figure 2. Experimental configuration: a) Schematic of the optical setup used to perform the imaging and spectroscopy. b) Confocal scan of the PL emission to locate a small cluster of PQDs. The emission from this small cluster of PQDs was coupled to the optical cavity for measurements. c) Bright field image of the curved features showing a bright fringe band that denotes mirror alignment. d) Curved features formed using FIB milling on a plinth of lateral dimensions 300 × 300 μm and a height of 100 μm. The emission was coupled to a curved feature with a radius of curvature 12 μm and depth 300 nm, which is shown in a black square box.

cavity modes by precisely moving the curved mirror toward the planar mirror using piezoelectric motion stages. At shorter cavity lengths ($\approx 1.2\mu$m), the mirrors were aligned to out-couple the cavity emission into a single TEM_{00} mode.

In Figure 1b, images (i) and (ii) are the transmission electron microscopy of monodispersed PQDs. The absorption spectrum of the PQDs (Figure 1c) shows a broad absorption range that allows their excitation with a broad range of wavelengths. The green shaded area in Figure 1c shows the free-space PL emission of the PQDs, which was obtained by exciting the spin-coated PQDs on the DBR as it faced the microscope objective. The DBR stop band (grey curve in Figure 1c) covered the entire PQD emission wavelength range. The free-space emission was fitted with a Lorentzian of full width at half maxima (FWHM) of 19.0 ± 2.0 nm. (see Section S1 (Supporting Information) for free-space PL measurements on multiple samples). This broad linewidth and isotropic free-space emission of PQDs make it difficult to design monochromatic LEDs or to couple it to other on-chip elements. Low temperatures environments reduce the linewidth, but even at cryogenic temperatures, the emission from clusters and single emitters remains relatively broad. Measuring this PQD batch at 7K, we found that PQDs clusters had an average linewidth of ≈5 nm, due to inhomogeneous broadening. See Section S2 (Supporting Information) for the PL measurements at cryogenic temperature in free-space configuration on multiple samples. Time-resolved photoluminescence measurements of free-space emission of PQDs shows a monoexponential decay lifetime of 2.48 ± 0.26 ns (Figure 1d).

Cavity alignment and photoluminescence measurements were performed using the setup shown in **Figure 2a**. CW 405 nm and pulsed 450 nm lasers were focused through a 0.70 NA air objective to confocally scan the sample (Figure 2b). The cavity was closed[42] using piezoelectric nanopositioning stages, and the cavity emission was directed to a single-photon avalanche detector (SPAD) and spectrometer. Figure 2c shows the plinth mirror with curved features during cavity alignment, where the bright fringe band passing through the centre of the image indicates the angle between the two cavity mirrors. The cavity length was monitored using spectral information. See Section S3 (Supporting Information) for details on using cavity interference fringes for angular alignment of two mirrors. The small total size and elevated geometry of the plinth (Figure 2d) facilitate alignment. Curved features with larger diameters increase mode volume, while smaller diameters that have lower mode volumes, increase the surface roughness. The optimum parameters we found were 12 μm ROC and 300 nm depth. This allowed us to achieve stable and low mode volumes that showed ultra-narrow linewidth single-mode emission (marked by a black square).

The cavity emission properties are depicted in **Figure 3**, where the cavity length was set to ≈1.20 μm. to obtain a low order longitudinal mode. This ensures a large free spectral range of more than 100 nm, which enables single mode emission from the cavity (see Section S4, Supporting Information). We measured emission from planar–planar mirror cavities (Figure 3a) and found that the cavity reduces the linewidth to 2.2 nm (vs 20 nm free-space linewidth). This reduction is insignificant as a cavity formed between two planar mirrors has large mode volume, which generates broad emission.[38,43,44] Practical applications demand low linewidth monochromatic mode emission, which can be obtained with concave-planar mirror cavities that produce sharp resonances. Figure 3b,c shows the emission from a concave-planar mirror cavity with a cavity length of 1.20 μm. The

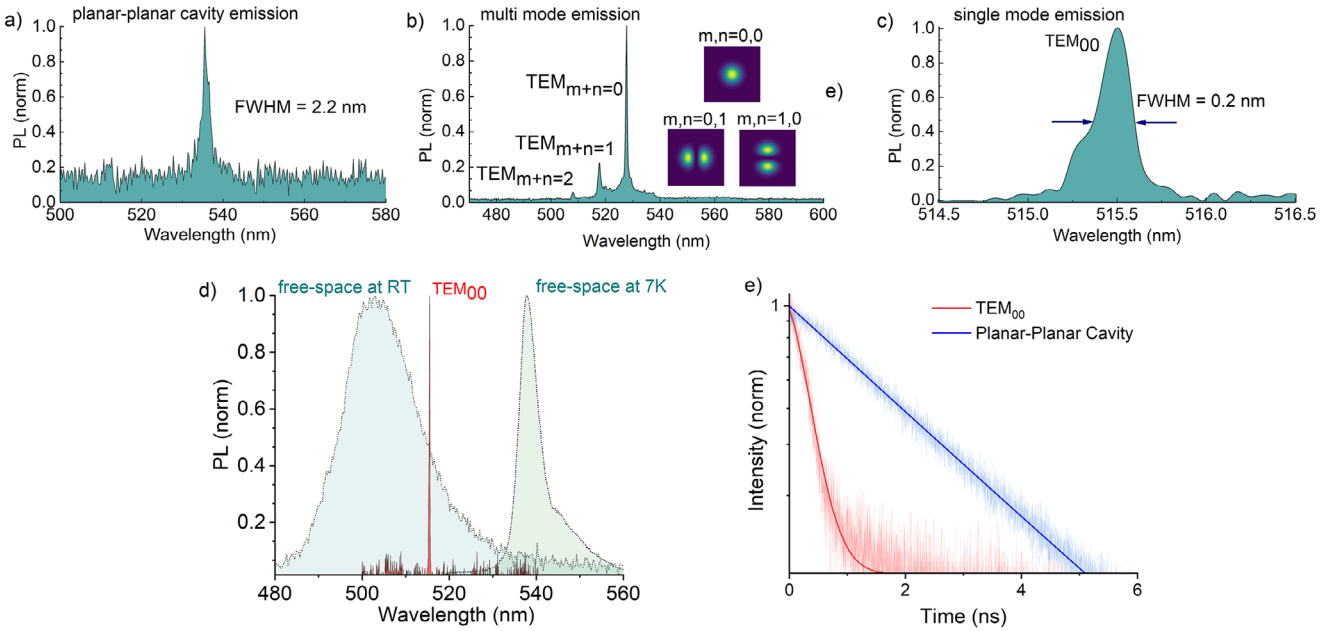

Figure 3. Room temperature single-mode ultra-narrow emission. a) PL emission from a cavity formed between the planar–planar region of the mirrors. The cavity re-shapes the emission profile and reduces the linewidth to 2.2 nm. b) Multimode emission from the cavity, formed between the concave and planar mirrors showing multiple HG modes with m and n values. c) Single TEM_{00} mode emission spectrum (smoothed) obtained after fine tuning the cavity alignment to couple the PQD emission to only a single mode. d) Single TEM_{00} mode emission from the cavity showing narrow linewidth emission as compared to the broad background emission from free-space emission and 5.4 nm linewidth emission from measurements at 7K. e) Time-resolved PL measurement and IRF deconvoluted fitting of the cavity-coupled emission for the planar–planar region (blue curves) and the TEM_{00} cavity mode formed between the concave and planar mirror (red curve) giving lifetimes of 2.37 and 0.13 ns, respectively.

modes supported by this system are Hermite–Gaussian (HG) modes with higher order solution, transverse modes, with the m and n as the eigenvalues of the Hermite Polynomials. Coupling of the emission with optical cavity modes can be seen in the collected PL from the cavity in Figure 3b. For a longitudinal mode, various transverse modes can be seen. For m = n = 0 the transverse electromagnetic (TEM) is the Gaussian mode profile, which is the most intense peak and has the lowest divergence.[38,45] Figure 3b shows small peaks corresponding to the outcoupling of individual transverse modes, each emitting at a different wavelength depending on the transverse mode indices m and n. Emission into the higher order eigenvalue modes have higher divergence, which makes it more difficult to couple the out-coupled emission into external optics. In the inset of Figure 3b, we show the calculated intensity distribution of the modes out-coupled from the cavity. See Section S5 (Supporting Information) for the beam profiles of higher order TEM modes. An in-plane mismatch between the emitter position and the concave mirror can force the emission into multiple transverse modes of a single longitudinal mode. These are the small peaks in Figure 3b. Optimum cavity alignment results in TEM_{00} modes as shown in Figure 3c. Theoretically, the emission from the emitters can be out-coupled to this single TEM_{00} mode with an efficiency of 0.54.[38,41,46] Figure 3c shows a zoomed-in spectral region of the TEM_{00} mode, depicting a linewidth of only 0.2 nm, which was limited by the resolution of our spectrometer. The actual emission linewidth can be <0.2 nm, which demonstrates the capability of our open-access optical cavity system. Thus, the cavity coupled emission shows a linewidth reduction of 100× as compared to the room temperature emission without any cryogenic cooling. This makes this system suitable for generating monochromatic light at room temperature.

To emphasise more on the practical application of our system, we compare the linewidth of our cavity-coupled emission to a cluster of PQDs at cryogenic temperature in Figure 3d. A cluster of PQDs shows a redshifted emission at lower temperatures[47–49] and exhibited a linewidth of 5.4 nm at 7K (Figure 3d), which reduces to <0.2 nm in the cavity system. Furthermore, we observed that at higher fluence with pulsed laser (110 mJ cm^{-2}) the lifetime of the emission coupled to the TEM_{00} mode decreases sharply to 0.13 ns showing the characteristics of the stimulated emission. At a comparable cavity length, the planar–planar section exhibits a longer lifetime of 2.37 ns, which is close to the off-cavity lifetime values. This similarity arises because these cavities do not offer significant Purcell enhancement at room temperature. These results highlight the potential of our experimental configuration as a robust scheme for delivering optical gain to emitters precisely placed at the resonance mode of the cavity.

Finally, to achieve lasing from the system, we pumped the cavity using a 405 nm continuous-wave (CW) laser source, gradually increasing the pump power. **Figure** 4a displays the variation in outcoupled emission from the cavity at three different input power densities. The gray curve corresponds to emission in the spontaneous regime at a pump power density of 120 W cm^{-2}, which is well below the lasing threshold. The cyan coloured curve represents emission near the threshold (157 W cm^{-2}), while the red curve illustrates stimulated emission above the threshold (200 W cm^{-2}), indicative of lasing behavior. These

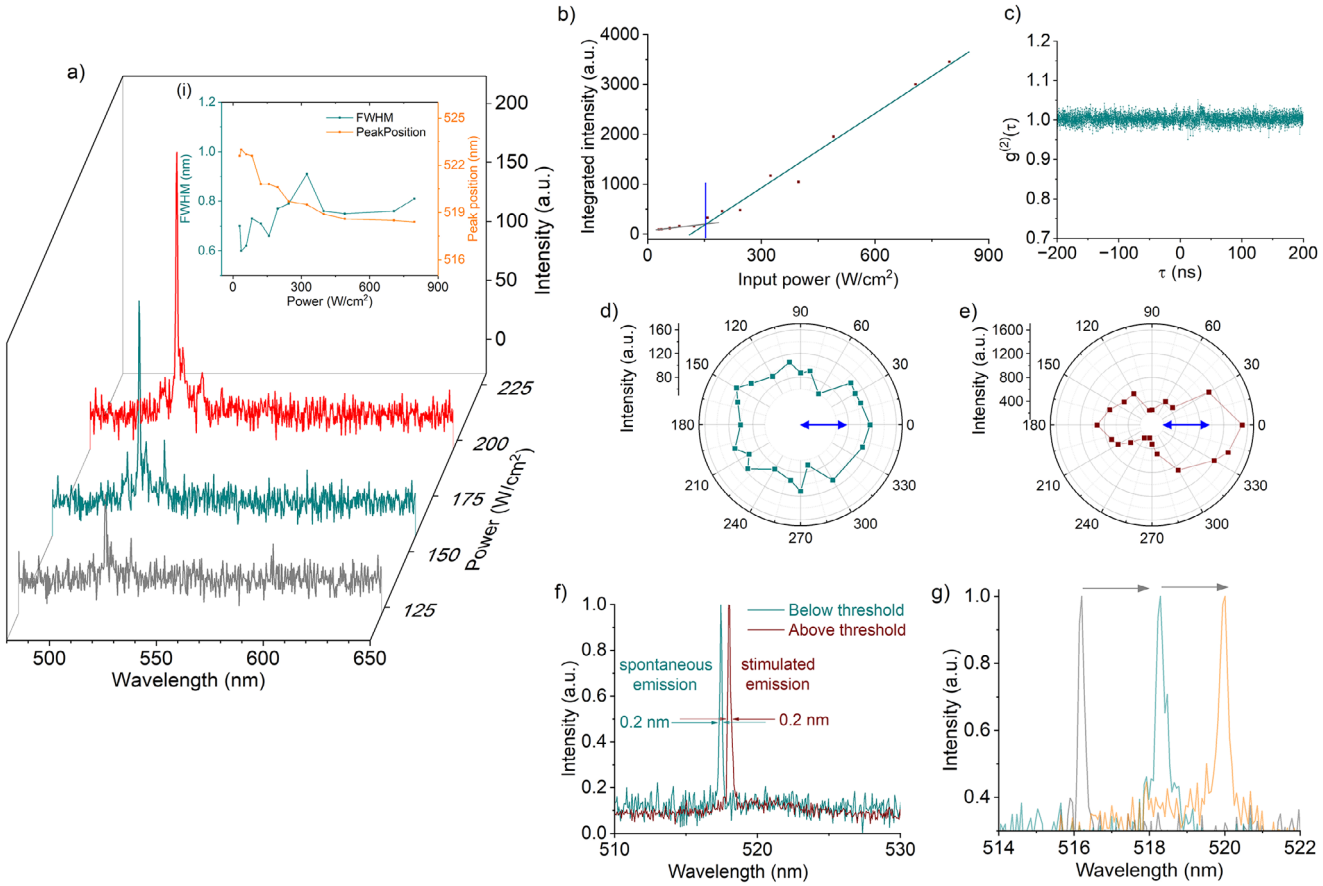

Figure 4. Continuous wave lasing from the cavity coupled PQDs. a) Intensity vs power curve for three different pump powers. Gray curve: below threshold (120 W cm^{-2}), Cyan curve: near the threshold (157 W cm^{-2}), and Red curve: above the lasing threshold (200 W cm^{-2}). Inset shows the stability of the FWHM and peak position of the lasing mode as a function of pumping power. b) Integrated intensity vs input power curve showing the transition of emission from spontaneous emission to lasing with a threshold of 152 W cm^{-2}. c) Second order correlation measurement of the emission from the cavity showing the coherence of the emission. d,e) Polarisation resolved emission from the cavity showing unpolarised emission below the threshold (≈30 W cm^{-2}) and polarised emission above the lasing threshold (≈200 W cm^{-2}) along the direction of incoming laser polarisation shown with blue arrow. f) Narrow spontaneous and lasing emission from the cavity showing single mode emission with Q values of 2585 and 2590 respectively. g) Fine tuning of the lasing mode wavelength by varying the cavity length.

regimes were identified by plotting the integrated intensity of the cavity's outcoupled emission as a function of input pump power density, as shown in Figure 4b. At low pump powers, the emission follows a sublinear trend characteristic of spontaneous emission. As the pump power increases, the emission exhibits a superlinear dependence, clearly revealing the threshold associated with the onset of lasing with a lasing threshold of 152 W cm^{-2}. Power-dependent measurements were carried out using a 300 grooves/mm grating to ensure high throughput, as prolonged measurements can cause slight cavity length shifts due to mechanical vibrations. Second order correlation measurements (Figure 4c) of the cavity emission above the lasing threshold (280 W cm^{-2}) show $g^2(0)$ value close to unity, indicating high coherence of the emission and ensuring the quality of the lasing mode. Polarisation resolved emission spectra (Figure 4d,e) shows the unpolarised emission from the cavity below the lasing threshold, and polarised emission above the lasing threshold along the direction of the incoming lasing polarisation (blue arrow along 0–180°) respectively. This effect arises because the linearly polarized pump mainly excites nanocrystal dipoles aligned along the pump polarization, initiating lasing in that direction. Above threshold, spontaneous symmetry breaking together with a small but finite mirror tilt lifts the cavity symmetry, causing the lasing polarization to follow the pump polarization, as also observed in similar microcavity systems.[50] Unlike other cavity designs where spontaneous emission is typically broad, our open-access cavity system constrains spontaneous emission to a linewidth limited by the cavity mode and spectrometer resolution, yielding an ultranarrow linewidth of 0.2 nm and a corresponding quality factor of 2590, as shown in Figure 4f. This narrowing of the emission is solely due to the coupling of the spontaneous emission to the curved-planar cavity modes, which also have been utilised recently by us to produce narrow linewidth single-photon source emission.[39] This demonstrates that the cavity structure not only narrows the emission linewidth but also defines the emission profile by coupling to the TEM_{00} modes of the cavity.

Upon increasing the pump power into the lasing regime, the linewidth and peak position remain stable, maintaining the same narrow spectral characteristics as shown in the inset of Figure 4a. A 1200 grooves/mm grating, with a resolution of 0.2 nm, was

used to characterize the emission in both regimes. For these measurements, the cavity was re-stabilized to allow for longer exposure times with the higher-resolution grating, which resulted in minor adjustments to the cavity length and thus the lasing wavelength. Switching to the lasing regime, the cavity wavelength remains stable while maintaining the linewidth of 0.2 nm and thus the quality factor of 2590 (Figure 4f, red curve), which is among the best reported values for VCSEL geometries using quantum dots (see Section S6, Supporting Information). This on-demand tunability of our open-access cavity design enables seamless switching between spontaneous and stimulated emission regimes while preserving ultra-narrow linewidths in both cases. The lasing emission remains quite stable as a function of time and decreases to 75% of its initial value in 450 s. This decay was observed to be a cumulative effect of both photodegradation of the emitters and the cavity drift as a function of time (see Section S7, Supporting Information). Though our cavity geometry enables coupling of the pristine PQDs emission to the cavity for modified spontaneous and stimulated emission, incorporating the emitters into a polymer matrix such as Polymethyl Methacrylate (PMMA) could further enhance their stability and lower the lasing threshold.[29] Furthermore, by changing the cavity length the lasing wavelength can be tuned precisely as shown in Figure 4g where the lasing mode was finely tuned from 516 to 520 nm without changing the pump power or the emitters location. For reproducibility and flexibility, we also observed lasing from a 450 nm CW laser, giving a lasing wavelength ≈530.1 nm as shown in Section S8 (Supporting Information). Such adaptability not only facilitates precision studies in quantum optics under spontaneous emission but also provides a scalable pathway for integrating low-threshold coherent light sources into next-generation nanophotonic and microphotonic devices.

3. Conclusion

To conclude, we have demonstrated ultranarrow spontaneous and lasing emission in a CW-pumped system by coupling the emission from PQDs to open-access, tunable dielectric optical cavities. Emission from the cavity-coupled mode outcoupled into a single transverse mode of the curved-planar cavities with an ultranarrow linewidth of 0.2 nm (limited by spectrometer resolution), yielding a quality factor of ≈2600—among the highest reported in a VCSEL-type design. The open-access architecture allows the emitters to remain in their native state without requiring a polymer matrix, while the tunable geometry overcomes the limitations of traditional VCSELs, which suffer from poor precision due to fixed mirror spacing. By precisely placing the emitters at the low-mode-volume regions of the curved-planar cavities, and pumping with a CW laser, lasing is achieved at a threshold of just 152 W cm^{-}2, without requiring pulsed excitation. Even at higher pump powers, the peak position and linewidth of the mode remain stable, indicating robust lasing and emitter stability. These results pave the way toward achieving CW polariton condensation in open cavities with real time tunability of the cavity length and coupling strength. Finally, the geometry can also be used with single photon emitters to achieve much narrower linewidths at room temperature, opening new possibilities for coherent light studies and quantum technological applications.

4. Experimental Section

Chemical Synthesis of $CsPbBr_3$ PQDs: All the chemicals, Cesium carbonate (Cs_2CO_3, 99.9%), lead bromide ($PbBr_2$, 99.9%), oleic acid (OA, technical grade, 90%), oleylamine (OAm, technical grade 770%), 1-octadecene (ODE, technical grade 90%), ethyl acetate (EtOAc, 99.5%), cyclohexane (anhydrous, 99.5%), and ethylene glycol (anhydrous, 99.8%), were purchased from Sigma–Aldrich and were used as received without any purification. $CsPbBr_3$ PQDs were synthesised using microwave-assisted preparation for achieving high-quality PQDs of the dimensions of ≈10nm. A 100 mL vial was used to prepare a mixture of Cs_2CO_3 (1 mmol, free 26 g), oleic acid (OA), and 60 mL of octadecene (ODE), with Cs_2CO_3 to OA molar ratios varying from 1:1 to 1:6. The solution was heated to 150°*C* and stirred until the Cs_2CO_3 fully dissolved, then allowed to cool to room temperature. Similarly, Pb precursors were prepared by combining $PbBr_2$ (1 mmol, 0.367 g) with OA, oleylamine (OAm), and 60 mL of ODE in another 100 mL vial. The ligands were added in different ratios (OA:OAm = 0:3, 0.5:2.5, 1:2, 1.5:1.5, 2:1, 2.5:0.5, and 3:0 mmol) with total loadings of ≈30, 34, 40, 45, and 60 mmol. This mixture was heated to 150°*C*, stirred for 1 h, and then cooled to room temperature. For the large-scale synthesis of $CsPbBr_3$ quantum dots, the reaction mixture was heated using a commercially available microwave (MW) oven (MW25B, LG Co.) in a specially designed quartz bath. The mixture underwent MW irradiation at 800 W for 5 min before being transferred to a 100 mL vial and cooled in an ice bath. After cooling, the solution was centrifuged at 8000 rpm for 10 min, and the resulting precipitate was dispersed in cyclohexane. This colloidal solution was then mixed with ethyl acetate and centrifuged at 5000 rpm for 5 min, after which it was re-dispersed in cyclohexane. This method successfully produced over 0.16 g of $CsPbBr_3$ quantum dots with excellent luminous properties from each 100 mL of reaction mixture. The Transmission electron microscopy was performed at 200 kV using HR-TEM; JEM-2100F, JEOL.

DBR and Curved Cavity Preparation: The DBRs were deposited on fused silica coverslips for fabricating planar and curved mirrors to minimize the autofluorescence of the glass. 11 pairs of SiO_2 and Ta_2O_5 layers, each with a thickness of a quarter wavelength, were deposited using the sputtering method. The reflectivity of the DBR were centered at a wavelength of 510 nm, which is near the emission maxima of the $CsPbBr_3$ PQDs. The thickness and the reflectivity of the SiO_2 layer and Ta_2O_5 layer are 86.1 and 58.5 nm, and 1.48 ± 0.01 and 2.18 ± 0.01, respectively. The curved mirrors were fabricated using FIB focused ion beam milling technique. A UV Fused Silica glass slide (Spectrosil 2000) was diced to make a plinth of lateral dimensions 300 × 300 μm and height of 100 μm. Various curved mirrors of radius of curvature (ROC) ranging from 5–25 μm and depth 300 and 600 nm were milled using FIB. For our experiments, a curved feature with ROC 12 μm and a depth of 300 nm was used to get low mode volume and high finesse.

Sample Preparation for the Optical Measurements: As prepared PQDs were diluted 100× and filtered through a 100 nm mesh to remove larger clusters. The filtered PQDs were then spin-coated onto a 10 mm diameter DBR-coated planar mirror at 1600 rpm for 60 s, followed by an increase to 2000 rpm for an additional 60 s to expedite drying. Afterward, the spin-coated mirror was mounted onto a sample holder, and a small emitter cluster was selected for cavity coupling using confocal scanning.

Experimental Setup: The imaging and spectroscopy of the cavity coupled PQDs were performed on a home-built confocal setup. The PQDs deposited on the planar mirror were excited either using a 405 CW or, using a 450 nm CW, or 450 nm pulsed laser (PicoQuant PDL-800D) with a 70 ps pulsed width and a repetition rate of 40 MHz. See Section S9 (Supporting Information) for the instrument response function (IRF). Both the planar, and curved mirror on plinths were placed on a custom-made sample holder attached to 3-axis Nanomax 300 piezoelectric stages. The curved mirror was placed on a Goniometric stage to fine tune the tilt for cavity alignment. The PQDs were excited using an infinity corrected 60x 0.70 NA objective lens (Olympus LUCPlanFLN) with a correction collar (0.1–1.3 mm) to account for the thickness of the DBR mirrors deposited on a coverslip. The laser was focused to a spot size of 2 µm on the front side of the planar mirror. The laser power was measured on the sample plane

after the objective lens. The emission from the cavity was collected using the same objective lens in the epi-fluorescence configuration. For the free-space measurements, the planar mirror with the dropcast PQDs was flipped such that the reflective side of the DBR mirror faced the objective lens. The beam was directed to the objective lens using a dichroic mirror (490 nm cut-off). The back reflected Rayleigh emission and the PL emission were transmitted through the dichroic mirror and were passed subsequently through long pass 480 and long pass 470 filters to remove the laser light completely. A 30:70 beam splitter (Thorlabs BSS10) was then used to direct the emission to the imaging camera and spectrometer. For second order correlation measurements, the signal was passed through additional filters (500 nm longpass and 550 nm shortpass), and was collected with a 50 μm 0.22 NA with 50:50 splitter optical fiber and subsequently analysed using two SPADs. For cavity alignment, the long pass filters were removed and a band pass filter 547/15 (Semrock TBP-01-547/15) was placed in front of the camera for better visibility of the fringes. Optical fibers of diameter 25 μm and 0.10 NA were used to perform the spectroscopy and TRPL measurements. A 0.3 m spectrometer with 10 μm slit width and 300 and 1200 grooves per mm gratings was used to perform the spectroscopy, with the light collected by a cooled CCD detector. TRPL measurements were performed using Micro Photon Devices SPADs and Time Tagger Ultra from Swabian Instruments. For low temperature measurements, the sample was cooled using a Janis ST-500 continuous flow liquid helium cryostat. The sample was excited at a wavelength of 405 nm with a Pulsed laser source (PicoQuant) at a repetition rate of 10 MHz using a 0.50 NA 100x objective lens (Mitutoyo).

Supporting Information

Supporting Information is available from the Wiley Online Library or from the author.

Acknowledgements

T.F. thanks the Gordon and Betty Moore Foundation, Lillian Martin and the Oxford Martin School. S.T. thanks Ryo Mizuta Graphics for providing the 3D Blender optical components, and the UK Research and Innovation (UKRI) under the Horizon Europe funding guarantee.

Conflict of Interest

The authors declare no conflict of interest.

Data Availability Statement

The data that support the findings of this study are available from the corresponding author upon reasonable request.

Keywords

dielectric cavities, lasing, narrow linewidth emission, perovskites

Received: June 14, 2025
Revised: November 4, 2025
Published online:

[1] J. Wang, F. Sciarrino, A. Laing, M. G. Thompson, *Nat. Photonics* **2020**, *14*, 273.
[2] K. Peters, J. Busink, P. Ackermans, K. Cognée, S. Rodriguez, *Phys. Rev. Res.* **2023**, *5*, 013154.
[3] A. B. Vasista, D. K. Sharma, G. Kumar, *arXiv preprint* **2018**, *arXiv:1806.08280* .
[4] W. Luo, L. Cao, Y. Shi, L. Wan, H. Zhang, S. Li, G. Chen, Y. Li, S. Li, Y. Wang, S. Sun, M. F. Karim, H. Cai, L. C. Kwek, A. Qun Liu, *Light: Sci. Appl.* **2023**, *12*, 175.
[5] L. Labonté, O. Alibart, V. D'Auria, F. Doutre, J. Etesse, G. Sauder, A. Martin, É. Picholle, S. Tanzilli, *PRX Quantum* **2024**, *5*, 010101.
[6] A. Y. Zhizhchenko, A. B. Cherepakhin, M. A. Masharin, A. P. Pushkarev, S. A. Kulinich, A. A. Kuchmizhak, S. V. Makarov, *Nano Lett.* **2021**, *21*, 10019.
[7] A. P. Schlaus, M. S. Spencer, K. Miyata, F. Liu, X. Wang, I. Datta, M. Lipson, A. Pan, X.-Y. Zhu, *Nat. Commun.* **2019**, *10*, 265.
[8] K. Koshelev, S. Kruk, E. Melik-Gaykazyan, J.-H. Choi, A. Bogdanov, H.-G. Park, Y. Kivshar, *Science* **2020**, *367*, 288.
[9] Z. Liu, J. Yang, J. Du, Z. Hu, T. Shi, Z. Zhang, Y. Liu, X. Tang, Y. Leng, R. Li, *ACS Nano* **2018**, *12*, 5923.
[10] L. Novotny, B. Hecht, *Principles of nano-optics*, Cambridge University Press, Cambridge, UK **2012**.
[11] M. Xie, C.-L. Tao, Z. Zhang, H. Liu, S. Wan, Y. Nie, W. Yang, X. Wang, X.-J. Wu, Y. Tian, *J. Phys. Chem. Lett.* **2022**, *13*, 2371.
[12] A. R. Dhawan, C. Belacel, J. U. Esparza-Villa, M. Nasilowski, Z. Wang, C. Schwob, J.-P. Hugonin, L. Coolen, B. Dubertret, P. Senellart, A. Maître, *Light: Sci. Appl.* **2020**, *9*, 33.
[13] A. Senichev, Z. O. Martin, S. Peana, D. Sychev, X. Xu, A. S. Lagutchev, A. Boltasseva, V. M. Shalaev, *Sci. Adv.* **2021**, *7*, eabj0627.
[14] J. Shamsi, P. Rastogi, V. Caligiuri, A. L. Abdelhady, D. Spirito, L. Manna, R. Krahne, *ACS Nano* **2017**, *11*, 10206.
[15] J. Leng, T. Wang, Z.-K. Tan, Y.-J. Lee, C.-C. Chang, K. Tamada, *ACS Omega* **2021**, *7*, 565.
[16] D. Di, K. P. Musselman, G. Li, A. Sadhanala, Y. Ievskaya, Q. Song, Z.-K. Tan, M. L. Lai, J. L. MacManus-Driscoll, N. C. Greenham, R. H. Friend, *J. Phys. Chem. Lett.* **2015**, *6*, 446.
[17] Y.-L. Hu, Q.-L. Wen, Z.-F. Pu, A.-Y. Liu, J. Wang, J. Ling, X.-G. Xie, Q.-E. Cao, *RSC Adv.* **2020**, *10*, 34215.
[18] G. M. Anilkumar, M. Bhakar, C. Taneja, S. Hwang, G. P. Kumar, G. Sheet, A. Rahman, *Adv. Mater.* **2024**, *36*, 2403875.
[19] C. Zhu, S. C. Boehme, L. G. Feld, A. Moskalenko, D. N. Dirin, R. F. Mahrt, T. Stöferle, M. I. Bodnarchuk, A. L. Efros, P. C. Sercel, M. V. Kovalenko, G. Rainò, *Nature* **2024**, *626*, 535.
[20] G. Ying, T. Farrow, A. Jana, H. Shao, H. Im, V. Osokin, S. B. Baek, M. Alanazi, S. Karmakar, M. Mukherjee, Y. Park, R. A. Taylor, *ACS photonics* **2021**, *8*, 2699.
[21] N. Toropov, G. Cabello, M. P. Serrano, R. R. Gutha, M. Rafti, F. Vollmer, *Light: Sci. Appl.* **2021**, *10*, 42.
[22] F. Montanarella, D. Urbonas, L. Chadwick, P. G. Moerman, P. J. Baesjou, R. F. Mahrt, A. Van Blaaderen, T. Stoferle, D. Vanmaekelbergh, *ACS Nano* **2018**, *12*, 12788.
[23] M. Reale, P. Castronovo, M. Cannas, E. Marino, A. Sciortino, F. Messina, *Adv. Opt. Mater.* **2025**, *13*, 2500838.
[24] M. B. Price, K. Lewellen, J. Hardy, S. M. Lockwood, C. Zemke-Smith, I. Wagner, M. Gao, J. Grand, K. Chen, J. M. Hodgkiss, E. L. Ru, N. J. L. K. Davis, *J. Phys. Chem. Lett.* **2020**, *11*, 7009.
[25] S. Laskar, A. C. Dakshinamurthy, S. Chithamallu, C. Sudarshan, C. Sudakar, *Opt. Lett.* **2023**, *48*, 2643.
[26] X. Li, K. Wang, M. Chen, S. Wang, Y. Fan, T. Liang, Q. Song, G. Xing, Z. Tang, *Adv. Opt. Mater.* **2020**, *8*, 2000030.
[27] X. Tian, L. Wang, W. Li, Q. Lin, Q. Cao, *ACS Appl. Mater. Interfaces* **2021**, *13*, 16952.
[28] Y. Wang, X. Li, V. Nalla, H. Zeng, H. Sun, *Adv. Funct. Mater.* **2017**, *27*, 1605088.

[29] H. Zhang, W. Wen, B. Du, L. Zhou, Y. Chen, S. Feng, C. Zou, L. Wu, H. J. Fan, W. Gao, H. Sun, J. Shang, T. Yu, *Nanoscale Horiz.* **2023**, *8*, 1403.
[30] C.-Y. Huang, C. Zou, C. Mao, K. L. Corp, Y.-C. Yao, Y.-J. Lee, C. W. Schlenker, A. K. Jen, L. Y. Lin, *Acs Photonics* **2017**, *4*, 2281.
[31] I. Georgakilas, D. Tiede, D. Urbonas, R. Mirek, C. Bujalance, L. Caliò, V. Oddi, R. Tao, D. N. Dirin, G. Rainò, S. C. Boehme, J. F. Galisteo-Lòpez, R. F. Mahrt, M. V. Kovalenko, H. Miguez, T. Stöferle, *Nat. Commun.* **2025**, *16*, 5228.
[32] C. Zou, X. Cao, Z. Wang, Y. Yang, Y. Lian, B. Zhao, D. Di, *Sci. Adv.* **2025**, *11*, eadr8826.
[33] J. Song, S. Ghosh, X. Deng, C. Li, Q. Shang, X. Liu, Y. Wang, X. Gao, W. Yang, X. Wang, et al., *Sci. Adv.* **2025**, *11*, eadr1652.
[34] C. Qin, A. S. Sandanayaka, C. Zhao, T. Matsushima, D. Zhang, T. Fujihara, C. Adachi, *Nature* **2020**, *585*, 53.
[35] Z. Li, J. Moon, A. Gharajeh, R. Haroldson, R. Hawkins, W. Hu, A. Zakhidov, Q. Gu, *ACS nano* **2018**, *12*, 10968.
[36] M. Ossiander, M. L. Meretska, S. Rourke, C. Spägele, X. Yin, I.-C. Benea-Chelmus, F. Capasso, *Nat. Commun.* **2023**, *14*, 1114.
[37] Z. Geng, J. Theenhaus, B. K. Patra, J.-Y. Zheng, J. Busink, E. C. Garnett, S. R. Rodriguez, *ACS photonics* **2021**, *8*, 1271.
[38] P. Dolan, S. Adekanye, A. Trichet, S. Johnson, L. Flatten, Y. Chen, L. Weng, D. Hunger, H.-C. Chang, S. Castelletto, *Opt. Express* **2018**, *26*, 7056.
[39] T. Farrow, A. R. Dhawan, A. R. Marshall, A. Ghorbal, W. Son, H. J. Snaith, J. M. Smith, R. A. Taylor, *Nano Lett.* **2023**, *23*, 10667.
[40] S. Cho, S. Hong, A. Jana, I. Han, H. Kim, H. Im, *J. Alloys Compd.* **2024**, *993*, 174700.
[41] L. Flatten, A. Trichet, J. Smith, *Laser Photonics Rev.* **2016**, *10*, 257.
[42] B. J. Ash, R. A. Nyman, J. M. Smith, A. A. P. Trichet, Optical microcavity device, alignment structure for an optical device, and method for aligning an optical device, **2022**, US Patent App. 17/764,939.
[43] S. Betzold, S. Herbst, A. A. Trichet, J. M. Smith, F. Wurthner, S. Hofling, C. P. Dietrich, *ACS Photonics* **2018**, *5*, 90.
[44] D. M. Coles, Y. Yang, Y. Wang, R. T. Grant, R. A. Taylor, S. K. Saikin, A. Aspuru-Guzik, D. G. Lidzey, J. K.-H. Tang, J. M. Smith, *Nat. Commun.* **2015**, *6*.
[45] W. T. Silfvast, *Laser fundamentals*, Cambridge university press, Cambridge, UK **2004**.
[46] S. Johnson, A. Watt, J. Smith, Ph.D. thesis, University of Oxford, Oxford, England **2015**.
[47] G. Mannino, I. Deretzis, E. Smecca, A. La Magna, A. Alberti, D. Ceratti, D. Cahen, *J. Phys. Chem. Lett.* **2020**, *11*, 2490.
[48] S. Yu, J. Xu, X. Shang, E. Ma, F. Lin, W. Zheng, D. Tu, R. Li, X. Chen, *Adv. Sci.* **2021**, *8*, 2100084.
[49] R. Saran, A. Heuer-Jungemann, A. G. Kanaras, R. J. Curry, *Adv. Opt. Mater.* **2017**, *5*, 1700231.
[50] C. P. Dietrich, A. Steude, L. Tropf, M. Schubert, N. M. Kronenberg, K. Ostermann, S. Höfling, M. C. Gather, *Sci. Adv.* **2016**, *2*, e1600666.